Fracture Mechanics of Concrete Structures,
Proceedings FRAMCOS-2, edited by Folker H. Wittmann,
AEDIFICATIO Publishers, D-79104 Freiburg (1995)

GRADIENT-ENHANCED SMEARED CRACK MODELS FOR FINITE ELEMENT ANALYSIS OF PLAIN AND REINFORCED CONCRETE

J.Pamin
Cracow University of Technology, Faculty of Civil Engineering, Poland
R. de Borst
Delft University of Technology, Faculty of Civil Engineering/ Eindhoven University of Technology, Faculty of Mechanical Engineering, the Netherlands

Abstract

A gradient-enhanced smeared crack model is utilised in finite element simulations of plain and reinforced concrete. It is rooted in a plasticity concept and uses a Rankine failure surface dependent on an equivalent fracture strain measure, as well as on its Laplacian. The loss of well-posedness of the boundary value problem at the onset of localisation is avoided, and finitely sized fracture process zones are obtained. A Double-Edge-Notched concrete specimen loaded in a combination of tension and shear is analysed and the results are verified against the experimental data. A reinforced concrete bar in uniaxial tension is calculated to evaluate the regularising influence on reinforced concrete structures.

1 Introduction

For a proper judgement of the structural safety of a system it is necessary to assess the danger of a sudden (brittle) failure after attaining the limit load. Structural concrete exhibits a softening behaviour due to non-homogeneous deformations resulting from cracking, Read & Hegemier (1984). Therefore, there exists a demand for reliable computational methods capable of reproducing the post-peak behaviour.

Classical, local constitutive models embody the implicit assumption that the deformation of the specimen varies in a sufficiently smooth manner. This is not the case when strain localisation occurs (e.g., when macrocracks develop during fracture). Nevertheless, a variety of smeared cracking, plasticity or damage based strain softening models exist, which feature a descending relation between stress and strain. The mathematical implication of such a constitutive relation within the classical continuum description is the loss of well-posedness of a given boundary value problem. The consequence in numerical simulations is a pathological discretisation sensitivity (e.g., Sluys, 1992).

To overcome this difficulty one can concentrate the damage evolution in a discontinuity (e.g. introduce discrete cracks between continuous parts of a concrete structure). Macroscopic cracking of concrete can then be reproduced, provided one knows the distribution of cracks in advance, Rots (1988), or performs frequent remeshing, Larsson & Runesson (1992). Otherwise a regularisation method must be applied within the continuum description in order to define the size of the localisation band or fracture process zone, de Borst et al. (1994), Willam et al. (1994), Pijaudier-Cabot et al. (1994). An intermediate solution, which removes the spurious mesh sensitivity from the load-displacement diagrams, is to treat the fracture energy as a material constant and to relate the softening modulus to the finite element size, cf. Pietruszczak & Mróz (1981), Bažant & Oh (1983), Willam (1984).

In the plasticity based smeared cracking model used here we adopt an enhanced continuum concept and define the failure surface as dependent on second-order spatial gradients of an inelastic strain measure. The gradient-dependent plasticity theory, cf. Aifantis (1984), Vardoulakis & Aifantis (1991), Mühlhaus & Aifantis (1991), de Borst & Mühlhaus (1992), Pamin (1994), preserves well-posedness of the boundary value problem during strain localisation and therefore spurious discretisation sensitivity of numerical results is avoided. The theory includes an additional parameter - the internal length scale, which is related to the width of the fracture band.

In this paper we focus on phenomenological modelling and the mesoscale effects of cracking are incorporated in a macroscopic constitutive model via the gradient dependence. For simplicity we adopt the strong assumptions of isotropy and a homogenised continuum. We use the gradient-dependent maximum principal stress (Rankine) failure surface and limit our consideration to the behaviour of concrete in plane stress tension and tension-shear. For a Double-Edge-Notched (DEN) concrete specimen a quantitative comparison with the experimental results has been carried out.

The problem of localisation and mesh sensitivity of numerical results is often thought to relate only to plain concrete. Nevertheless, problems also exist for reinforced concrete when cracking is modelled using standard continuum models, since the crack spacing in then undefined. To investigate the possible beneficial effects of adding spatial gradients to the smeared crack model a reinforced concrete specimen in uniaxial tension is analysed.

2 Plasticity-based smeared crack model

The gradient-dependent plasticity theory is used to simulate continuum fracture, cf. de Borst et al. (1992), Pamin & de Borst (1994). Although plasticity is a more natural constitutive description for metals and soils, it enables modelling of the characteristic features of quasi-brittle (cementitious) materials under monotonic loading conditions, Feenstra (1993). Incapability of reproducing the elastic stiffness degradation cannot be accepted for cyclic loading, for which a damage theory, see e.g. Pijaudier-Cabot et al. (1994), or a combination of damage and plasticity, see e.g. Larsson & Runesson (1994), is more appropriate. It is also noted that the isotropic softening plasticity model is not correct for concrete cracking, cf. Feenstra (1993), since in reality the emergence of a crack does not reduce the local material strength in all directions, but only in the direction perpendicular to the crack. However, here we focus attention on the role of the gradient regularisation in enhancing the classical smeared cracking model and we accept these limitations.

The maximum principal stress (Rankine) criterion, adopted as a condition of continuum fracture, is formulated here for the plane stress case:

$$F = \sigma_1 - \bar{\sigma}_{\mathrm{g}}(\kappa\,, \nabla^2 \kappa)\ , \tag{1}$$

where σ_1 is the maximum principal stress and $\bar{\sigma}_{\mathrm{g}}$ is the gradient dependent fracture strength. For this fracture criterion the equivalent inelastic strain rate $\dot{\kappa}$ is defined as the absolute value of the maximum principal inelastic strain rate $\dot{\varepsilon}^{\mathrm{p}}_1$.

The Rankine failure surface for plane stress conditions possesses a vertex $\boldsymbol{\sigma}_{\mathrm{v}} = (\bar{\sigma}, \bar{\sigma}, 0)$ in the space $(\sigma_x\,, \sigma_y\,, \sigma_{xy})$. For classical plasticity algorithms the presence of vertices in yield functions involves already some extra difficulties, cf. Koiter (1953), de Borst (1987), Simo et al. (1988). The situation is different in the gradient plasticity algorithm, where the plastic multiplier is discretised. A possible, but expensive solution is to introduce the discretisation of more than one plastic multiplier in the element formulation and penalise all of them but one to zero, unless the vertex regime is entered. The second approach, followed in this paper, is to apply a smooth approximation of the original failure function, Pamin (1994).

Next, we consider some gradient-dependent softening rules. We introduce a nonlinear softening rule

$$\bar{\sigma}_{\mathrm{g}}(\kappa, \nabla^2 \kappa) = \bar{\sigma}(\kappa) - g(\kappa) \nabla^2 \kappa\ , \tag{2}$$

in which $\bar{\sigma}(\kappa)$ is a given exponential softening rule (e.g. as in Fig. 1) and $g(\kappa)$ is a given gradient influence function. We assume that $\bar{\sigma}_{\mathrm{g}} \geq 0$. The softening function according to Hordijk (1991), formulated originally in the context of discrete cracking under uniaxial tension, has been adapted here to the continuum format using the relation:

$$\frac{G_{\mathrm{f}}}{w} = \int \sigma \,\mathrm{d}\varepsilon = \int \bar{\sigma}\,\mathrm{d}\kappa\ , \tag{3}$$

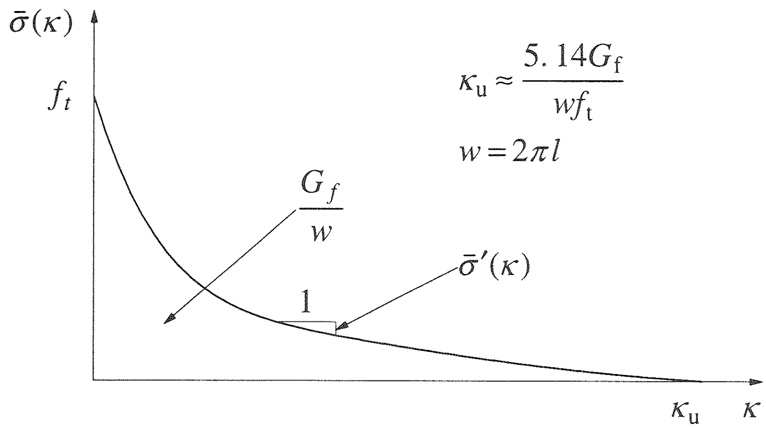

Fig. 1. Nonlinear softening rule for concrete Mode-I fracture, cf. Hordijk (1991).

where G_f is the fracture energy and w is the crack band width. The relation between w and the internal length l is assumed to be similar to the uniaxial analytical solution, de Borst & Mühlhaus (1992). We generalise the relation between the gradient influence variable g, the classical hardening modulus $\bar{\sigma}'$ and the length scale l, found for the analytical solution and linear softening, to the case of nonlinear softening

$$g(\kappa) = -l^2 \bar{\sigma}'(\kappa) \,, \tag{4}$$

with l constant and $\bar{\sigma}' < 0$, Pamin (1994). The gradual failure of crack grain bridges which produce the residual carrying capacity of concrete, van Mier (1991), suggests that the gradient influence should decrease with the increase of the accumulated fracture strain. This leads to the following gradient-dependent softening rule:

$$\bar{\sigma}_g(\kappa \,, \nabla^2 \kappa) = \bar{\sigma}(\kappa) + l^2 \bar{\sigma}'(\kappa) \nabla^2 \kappa \,. \tag{5}$$

The simplest case is to assume linear softening ($h = \bar{\sigma}'$ = constant) and a constant gradient influence coefficient g:

$$\bar{\sigma}_g(\kappa, \nabla^2 \kappa) = \sigma_y + h\kappa - g \nabla^2 \kappa \,. \tag{6}$$

The gradient-dependent yield strength in eq. (2) is composed of two contributions. The gradient contribution $-g(\kappa)\nabla^2\kappa$ is positive in the middle of the localisation band, giving additional carrying capacity to the gradient-dependent material in this area, i.e. even if $\bar{\sigma}$ equals zero, the yield strength $\bar{\sigma}_g$ is larger than zero. The case of a negative gradient contribution occurs at the elastic-plastic boundary, making it possible for the localisation zone to spread, since the elastic elements close to the elastic-plastic boundary have an apparent reduced yield strength. These modifications of the standard yield strength $\bar{\sigma}(\kappa)$ are the essence of the gradient regularisation.

3 Fracture of the DEN-specimen

Fig. 2 shows the configuration of a mixed-mode concrete fracture test, analysed experimentally by Nooru-Mohamed (1992). The Double-Edge-Notched specimen was placed in a special loading frame that allowed for the analysis of various loading paths of combined shear and tension under force or deformation control. We have analysed two of the loading paths considered by Nooru-Mohamed (1992) using the gradient-enhanced smeared crack model.

Three specimen sizes ($L \times L$) were used in the experiments: 200×200, 100×100, 50×50mm. The sizes of symmetrical notches were 25×5, 12.5×5 and 6.25×5mm, respectively, and the specimen thickness was for all cases $t=50mm$. The material data used in numerical simulations are as follows: Young's modulus $E=30000\,N/mm^2$, Poisson's ratio $\nu=0.0$, tensile strength $f_t \approx 3.00\,N/mm^2$, fracture energy $G_f=0.10\,N/mm$. The non-linear softening rule from Fig. 1 and the internal length $l=2mm$ ($\kappa_u=0.0136$) have been assumed.

In Fig. 2 we have presented the geometry of the specimen 200×200mm and the finite element mesh used in the calculations. The central zone of refined mesh ($50 \le y \le 150$) is composed of eight-noded gradient plasticity elements (quadratic interpolation of displacements and hermitian interpolation of the plastic multiplier) and the coarse mesh zones at the top and at the bottom are discretised with standard serendipity elements. Additional boundary conditions for the plastic multiplier field are enforced on the boundaries of the fine mesh and the respective displacements are tied on the remeshing lines to preserve the displacement continuity.

The specimen in Fig. 2 is used in the first series of simulations. According to path 4 from the experiment, the shear force is applied under force control and then kept constant, while the normal loading is imposed under displacement control of the normal deformation in the fracture zone δ (averaged value measured between the points A and A' as well as between B and B'). In the second series all three sizes are analysed to verify the size effect. To obtain a monotonic increase of loading, the shear and tension are applied simultaneously under the control of the horizontal and vertical displacements p_s and p with the condition $p=p_s$. It is noted that this deformation control is only a numerically convenient approximation of the real case, since in the experiment (path 6) the relative shear deformation between the upper and lower half of the specimen δ_s (measured at the points S and S') and δ were used to control the loading.

Fig. 3 shows the experimentally determined and numerically simulated relations between the tensile load P and the normal displacement δ. The calculated maximum shear load $P_{s\max}=29.7kN$ is larger than the experimental value (about 27.5kN) and the ultimate carrying capacity under subsequent tension is even stronger overestimated, which is attributed to the stress locking in the notch area and overestimation of the cracking stress in

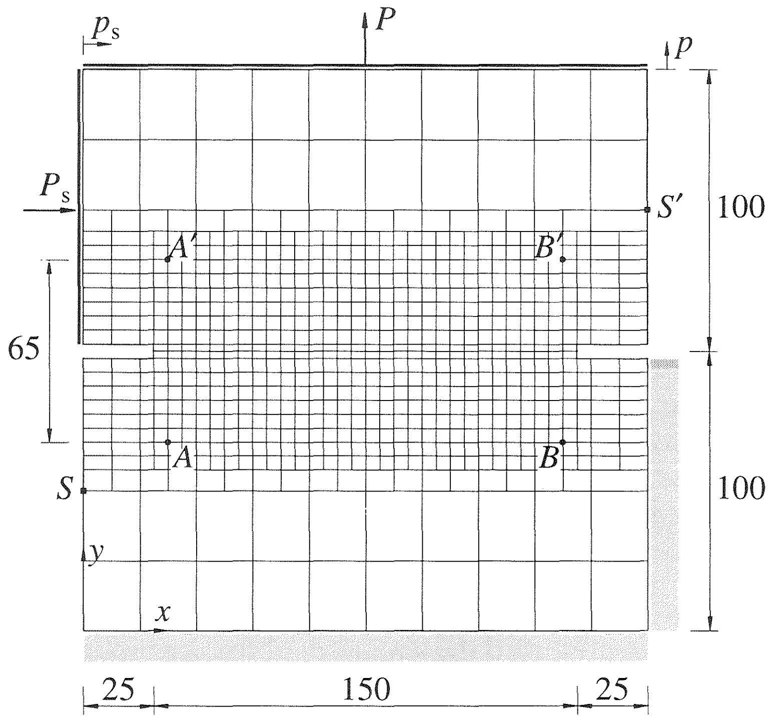

Fig. 2. Double-edge-notched concrete specimen with discretisation.

the presence of the lateral compression. On the other hand, the character of the experimental curves is correctly reproduced and the results are close to experiments for progressive softening.

The simulated fracture process zones are compared in Fig. 4 with the average experimental crack positions, i.e. an average of the experimental crack locations at the front and back of the specimen is plotted. The agreement is reasonable and no bias of the mesh lines is found as was the case in the smeared cracking simulations, cf. Nooru-Mohamed (1992). It is noted that for the case with $P_{s\,max}$ the central zone of gradient plasticity elements had to be extended over the area $40 \leq y \leq 160$ in order to admit the inclined 'crack' propagation. For the case $P_s = 5kN$ two fracture zones developing from the notches finally join, for the other cases the width of the compressive strut is estimated correctly. The width of the fracture zones corresponds well to the assumed value $w = 2\pi l \approx 12.6mm$.

In the presence of localisation the stress-strain relation is only a nominal property and structural effects (like the size effect) have to be reflected. It has been shown in the context of concrete fracture, that the deterministic size effect - due to the release of the stored elastic energy - is much more important than the probabilistic size effect, due to the randomness of the material strength, cf. Bažant (1992). In contradiction to the classical models we are capable of reproducing the deterministic size effect since the length parameter is incorporated in the theory.

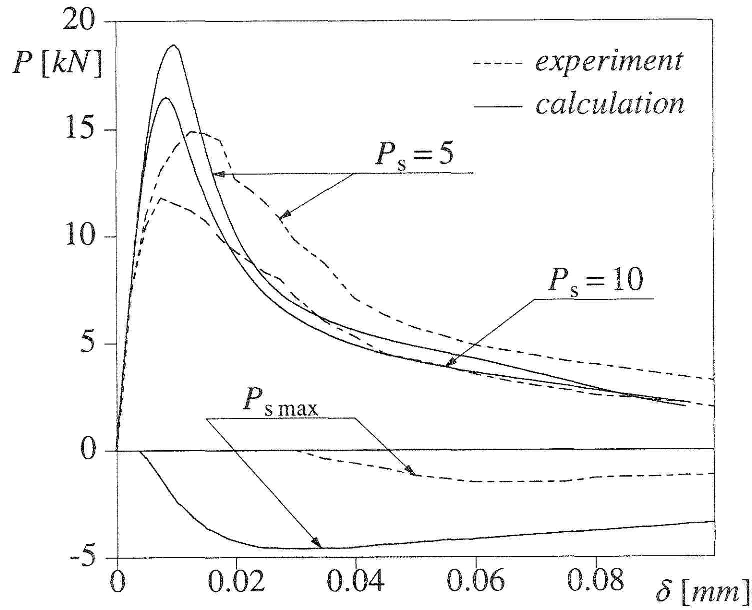

Fig. 3. Computed and experimental tensile force versus average normal displacement diagrams (path 4).

In the second series of calculations we have applied simultaneously equal shear and tensile deformation (path 6). Fig. 5 shows the calculated diagrams for the relation between the nominal stress $P/(tL_0)$, where L_0 is the load carrying length equal to 150, 75 and 37.5*mm* for the three respective specimen sizes, and the average normal strain (δ/L). For the smaller specimens two possibilities are considered: a changing internal length $l = 1/0.5mm$ (so that $l/L = 0.01$) and a constant internal length $l = 2mm$. For all cases the fracture energy G_f is the same.

As can be seen in Fig. 6 the choice of the internal length can influence the predicted fracture mode. If the internal length is decreased together with the specimen size, two cracks are predicted for all three specimens. If the internal length is kept constant, we find just one fracture zone for the medium and small specimen. It is noted that in the experiments both crack patterns, distributed and with dominant cracks, were observed in the series of medium and small specimens. From Fig. 5 we observe, that the choice of the internal length influences the softening behaviour. A classical size effect is found both in the peak-stress value and the post-peak regime although in the experiment a reversed size effect was found for path-6 tests. Since an internal length scale is incorporated in the numerical model, the predicted size effect law need not be a power law and our results correspond to the predictions of nonlinear elastic fracture mechanics, cf. Bažant (1992), Reinhardt & Ožbolt (1994).

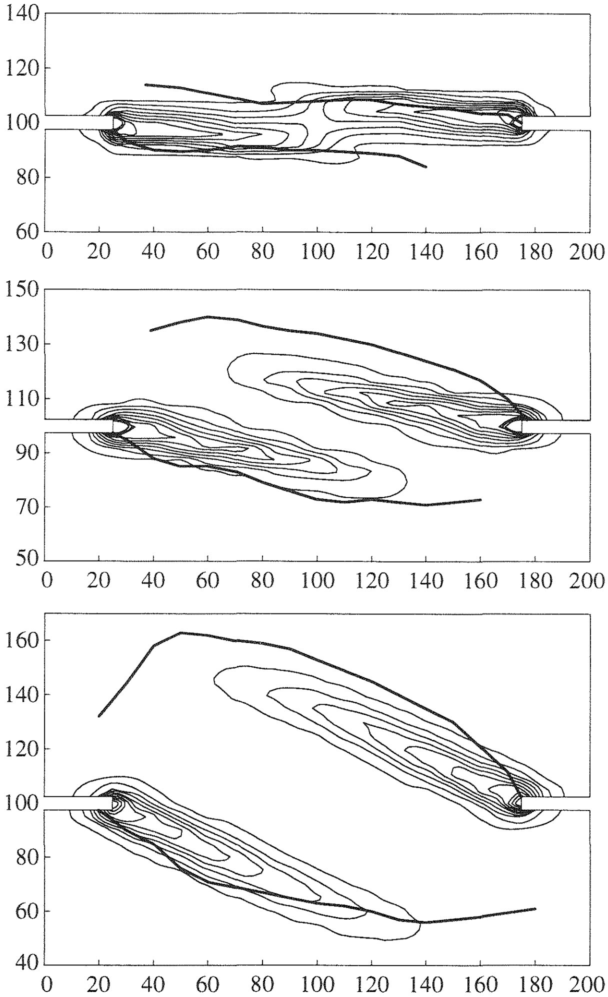

Fig. 4. Contour plots of equivalent fracture strain for the three lateral confining load levels (from the top $P_s = 5, 10, P_{s\,max}$).

4 Cracking of the RC tensile bar

We analyse numerically the reinforced concrete bar in tension shown in Fig. 7. The following geometrical and material data have been used: length of the bar $L = 100\,mm$, $E = 20000\ N/mm^2$ and $f_t = 2\ N/mm^2$ for concrete, $E = 210000\ N/mm^2$ and $\sigma_y = 500\ N/mm^2$ for the steel (ideal plasticity).

First, we have adopted the embedded reinforcement formulation, in which the deformations of the steel rod and the concrete matrix are equal, i.e. full bond is assumed. Eighty eight-noded gradient plasticity elements, linear softening modulus $h = -0.1\,E$ and internal length $l = 5\ mm$ are used (resulting in a width of the localisation zone $w = 31.4\ mm$). To initiate cracking we have introduced a small imperfection (reduced value of the fracture strength) in the centre of the bar. We have obtained the load-

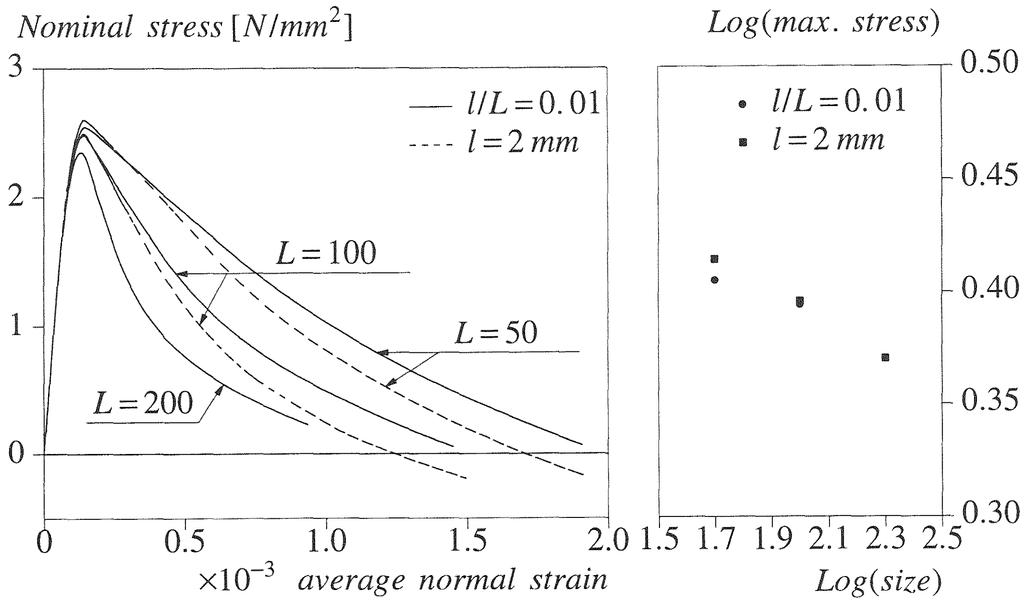

Fig. 5. Nominal tensile stress versus average tensile strain diagram and the size effect on the peak-stress (path 6).

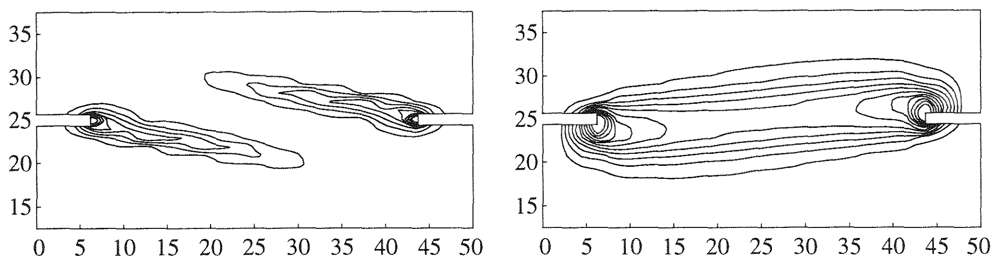

Fig. 6. Contour plots of equivalent fracture strain for the smallest specimen and different internal length values: $l=0.5mm$ (left) and $l=2mm$ (right).

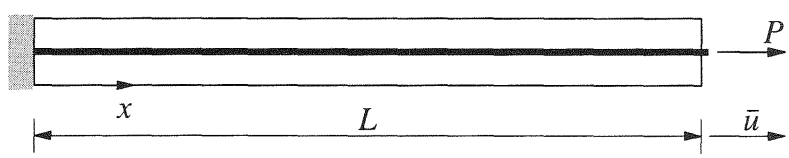

Fig. 7. Reinforced concrete bar in pure tension.

deformation diagrams and inelastic strain distributions for three reinforcement ratios, $\mu=0.5, 1.0, 2.0\%$, see Fig. 8, as well as the case with no reinforcement.

The stabilising influence of the reinforcement is clearly observed, but

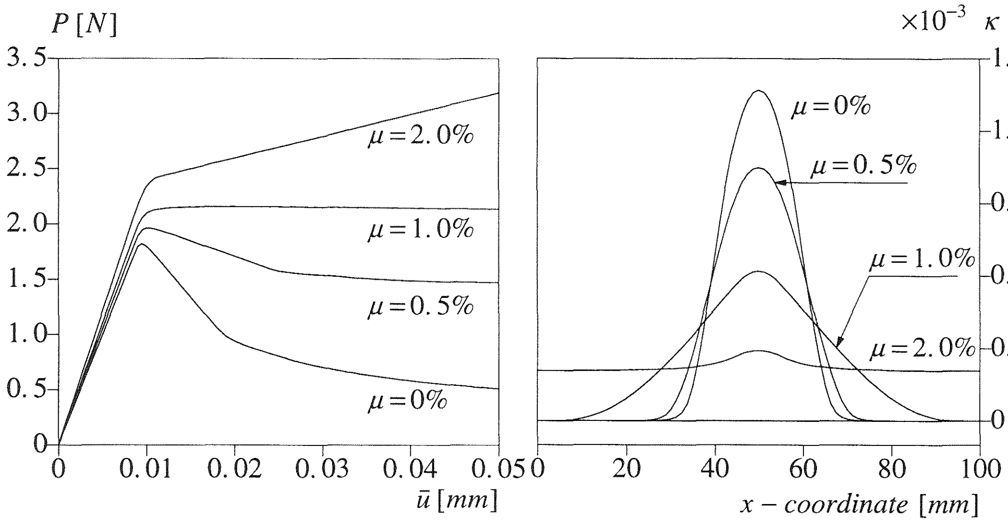

Fig. 8. Load-displacement diagrams for different reinforcement ratios and the fracture strain distributions in the bar at $\bar{u}=0.03mm$.

for $\mu=0.5\%$ a localized fracture zone is still possible. For plain concrete the stresses along the bar are constant, for reinforced concrete the stresses in the fracture zone are transferred to the reinforcement, but outside of this zone the stresses are constant. The response of the numerical model is different if the bond slip is taken into account. The crack formation is associated with a slip and stress redistribution between concrete and steel. At a distance from the primary crack the stresses mobilise and violate the cracking criterion again.

This is illustrated using a numerical model with 80 gradient plasticity elements for concrete, 80 interface elements which reproduce the bond slip law of Dörr (1980) and 80 truss elements for steel. The imperfection in now placed at the left end of the bar and nonlinear softening with the ultimate inelastic strain $\kappa_u=0.006$ is assumed. For the reinforcement ratio $\mu=2.0\%$ and two values of the internal length we have obtained the inelastic strain distributions in Fig. 9. For $l=3mm$ we observe two discrete cracks and for $l=5mm$ we have a zone of distributed fracture. Fig. 10 presents the evolution of the stress distributions in the reinforcement and the interface for $l=3mm$.

These results show that localisation and formation of multiple discrete cracks can occur even for strongly reinforced concrete. However, the results do not seem to be sufficient to support the conclusion of Sluys (1994) and Brioschi (1994), obtained in wave-propagation tests, that the internal length scale determines the crack spacing. To verify this a longer bar must be analysed and a careful parametric study must be carried out, since a number of factors (e.g. reinforcement ratio, bond strength and softening diagram) may influence the results.

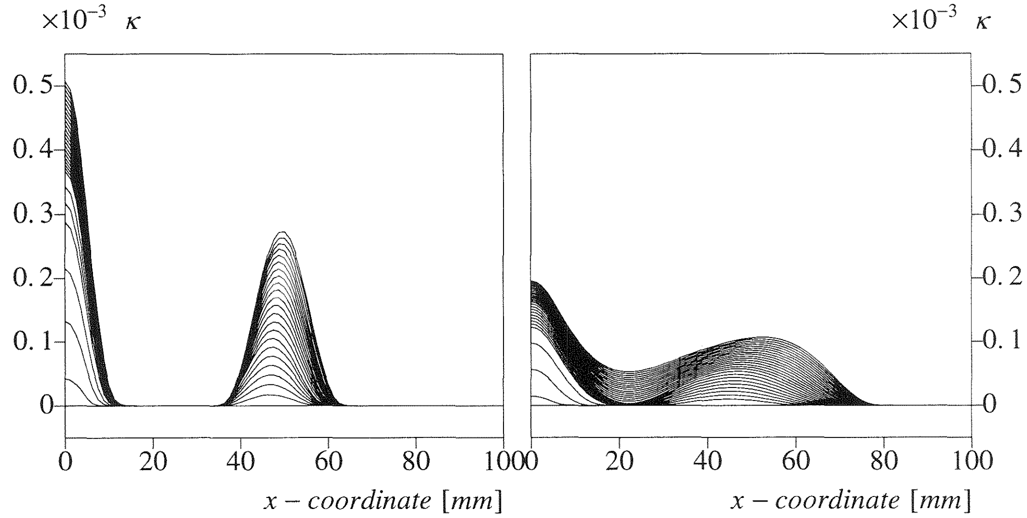

Fig. 9. Evolution of the fracture strain in the bar for two values of the internal length $l = 3mm$ and $l = 5mm$ ($\bar{u} = 0 \rightarrow 0.02mm$).

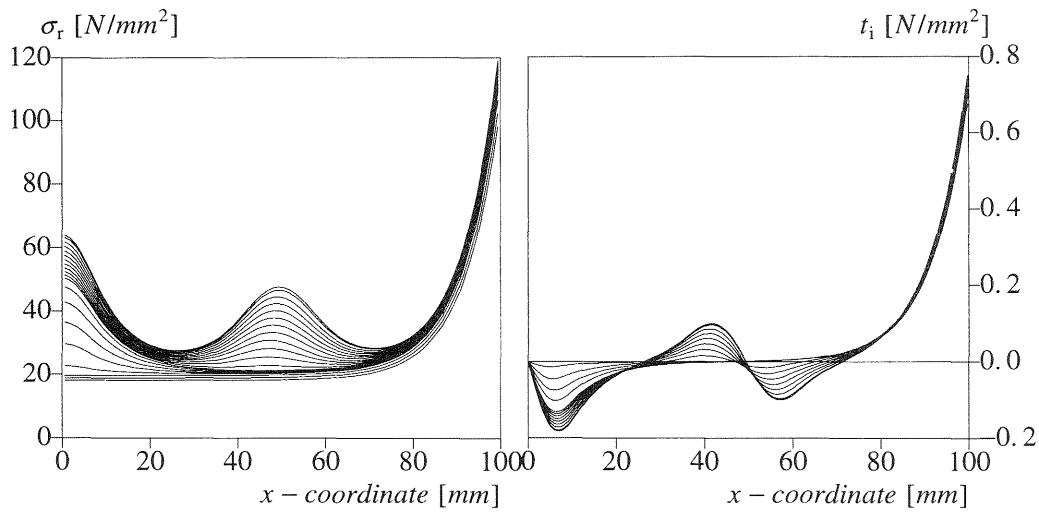

Fig. 10. Evolution of stresses in the reinforcement (left) and tractions in the interface (right) for $l = 3mm$ ($\bar{u} = 0 \rightarrow 0.02mm$).

5 Final remarks

In this paper the applicability of a gradient-enhanced smeared crack mode for plain and reinforced concrete has been scrutinised. The employed plasticity approach includes a regularising dependence of the failure function on higher-order spatial derivatives of an inelastic strain measure and therefore the boundary value problem for a softening continuum remains well-posed in the post-peak regime.

We have shown that the crack model based on Rankine gradient plasticity may be successfully applied in the analysis and prediction of concrete fracture phenomena. The model reproduces the experimentally observed structural response. The results of finite element simulations are almost insensitive to mesh refinement or alignment, since the width of the fracture process zones is determined by the internal length incorporated in the theory. The load-deformation diagrams for the DEN-specimen are governed by the value of fracture energy and are not affected by the assumed value of the internal length, unless its change results in a different localisation mode. However, the model seems to be less accurate for this mixed-mode fracture problem than for the pure Mode-I cases, cf. Pamin (1994). The localisation limiting properties of the gradient enhancement make the results physically appealing, although the curved shape of the experimentally observed cracks has not been reproduced satisfactorily.

The issue of modelling of localisation in reinforced concrete requires a more extensive study, in which the effect of bond slip is of primary importance. In particular the use of a continuum theory equipped with an internal length parameter can make it possible to determine the crack spacing and the minimum reinforcement ratio necessary to obtain distributed cracking. It is also emphasised that the experimental or micromechanical determination of the internal length scale (or rather a set of length scales for different stress states) for various materials is of primary importance.

6 Acknowledgements

Financial support from the Commission of the European Communities through the HCM project A.L.E.R.T. "Geomaterials", and from the Polish Committee of Scientific Research within project no 3 P404 060 06 is gratefully acknowledged. The authors also wish to record their gratefulness to Dr. L.J. Sluys and Dr. A. Winnicki for illuminating discussions and useful suggestions.

References

Aifantis, E.C. (1984) On the microstructural origin of certain inelastic models. **J. Eng. Mater. Technol.,** 106, 326-330.

Bažant, Z.P. and Oh, B. (1983) Crack band theory for fracture of concrete. **RILEM Materials and Structures,** 16, 155-177.

Bažant, Z.P. (1992) Scaling laws in mechanics of failure. **ASCE J. Eng. Mech.,** 119, 1828-1845.

de Borst, R. (1987) Integration of plasticity equations for singular yield functions. **Comp. & Struct.,** 26, 823-829.

de Borst, R. and Mühlhaus, H.-B. (1992) Gradient-dependent plasticity: Formulation and algorithmic aspects. **Int. J. Num. Meth. Eng.,** 35, 521-539.

de Borst, R., Mühlhaus, H.-B. and Pamin, J. (1992) A gradient continuum model for Mode-I fracture in concrete and rock, in **Fracture Mechanics of Concrete Structures** (ed. Z.P. Bažant), Elsevier Applied Science, London and New York, 251-259.

de Borst, R., Feenstra, P.H., Pamin, J. and Sluys, L.J. (1994) Some current issues in computational mechanics of concrete structures, in **EURO-C 1994**

Int. Conf. Computer Modelling of Concrete Structures (eds H. Mang et al.), Pineridge Press, Swansea, 283-302.
de Borst, R., Pamin, J. and Sluys, L.J. (1995) Gradient plasticity for localization problems in quasi-brittle and frictional materials, in **Proc. Fourth Int. Conf. Computational Plasticity: Fundamentals and Applications,** (eds D.R.J. Owen et al.), Pineridge Press, Swansea, 509-533.
Brioschi, M.A. (1994) Dynamic failure in reinforced concrete elements. **TU Delft Report** no 03.21.1.31.19, Delft University of Technology, Delft.
Dörr, K. (1980) Ein Beitrag zur Berechnung von Stahlbetonscheiben unter besonderer Berücksichtigung des Verbundverhaltens. **Dissertation,** University of Darmstadt, Darmstadt.
Feenstra, P.H. (1993) Computational aspects of biaxial stress in plain and reinforced concrete. **Dissertation,** Delft University of Technology, Delft.
Hordijk, D.A. (1991) Local approach to fatigue of concrete. **Dissertation,** Delft University of Technology, Delft.
Koiter W.T. (1953) Stress-strain relations, uniqueness and variational theorems for elastic-plastic materials with a singular yield surface. **Q. Appl. Mech.,** 11, 350-354.
Larsson, R. and Runesson, K. (1992) Plastic localisation captured by discontinuous displacement approximation, in **Proc. Third Int. Conf. Computational Plasticity: Fundamentals and Applications** (eds D.R.J. Owen et al.), Pineridge Press, Swansea, 605-616.
Larsson, R. and Runesson, K. (1994) Cohesive crack models derived from localization and damage coupled to plasticity, in **EURO-C 1994 Int. Conf. Computer Modelling of Concrete Structures** (eds H. Mang et al.), Pineridge Press, Swansea, 413-424.
van Mier, J.G.M. (1991) Mode-I fracture of concrete: discontinuous crack growth and crack interface grain bridging. **Cement and Concrete Research,** 21, 1-15.
Mühlhaus, H.-B. and Aifantis, E.C. (1991) A variational principle for gradient plasticity. **Int. J. Solids Structures,** 28, 845-857.
Nooru-Mohamed, M.B. (1992) Mixed-mode fracture of concrete: an experimental approach. **Dissertation,** Delft University of Technology, Delft.
Pamin, J. (1994) Gradient-dependent plasticity in numerical simulation of localization phenomena. **Dissertation,** Delft University of Technology, Delft.
Pamin, J. and de Borst, R. (1994) Gradient plasticity and finite elements in the simulation of concrete fracture, in **EURO-C 1994 Int. Conf. Computer Modelling of Concrete Structures** (eds H. Mang et al.), Pineridge Press, Swansea, 393-402.
Pietruszczak, St. and Mróz, Z. (1981) Finite element analysis of deformation of strain-softening materials. **Int. J. Num. Meth. Eng.,** 17, 327-334.
Pijaudier-Cabot, G., La Borderie, Ch. and Fichant, S. (1994) Damage mechanics for concrete modelling: Applications and comparisons with plasticity and fracture mechanics, in **EURO-C 1994 Int. Conf. Computer Modelling of Concrete Structures** (eds H. Mang et al.), Pineridge Press, Swansea, 17-36.
Read, H.E. and Hegemier, G.A. (1984) Strain softening of rock, soil and concrete - A review article. **Mech. Mater.,** 3, 271-294.
Reinhardt, H.W. and Ožbolt, J. (1994) Concrete mechanics aspects as background for structural modelling, in **DIANA Computational Mechanics '94** (eds G.M.A. Kusters and M.A.N. Hendriks), Kluwer Academic Publishers, Dordrecht, 57-67.

Rots, J.G. (1988) Computational modeling of concrete fracture. **Dissertation,** Delft University of Technology, Delft.
Simo, J.C., Kennedy, J.G. and Govindjee, S. (1988) Non-smooth multisurface plasticity and viscoplasticity. Loading/unloading conditions and numerical algorithms. **Int. J. Num. Meth. Eng.,** 26, 2161-2185.
Sluys, L.J. (1992) Wave propagation, localization and dispersion in softening solids. **Dissertation,** Delft University of Technology, Delft.
Sluys, L.J. (1994) Dynamic failure in reinforced concrete structures, in **DIANA Computational Mechanics '94** (eds G.M.A. Kusters and M.A.N. Hendriks), Kluwer Acadamic Publishers, Dordrecht, 193-203.
Vardoulakis, I. and Aifantis, E.C. (1991) A gradient flow theory of plasticity for granular materials. **Acta Mechanica,** 87, 197-217.
Willam, K.J. (1984) Experimental and computational aspects of concrete fracture, in **Int. Conf. Computer Aided Analysis and Design of Concrete Structures** (eds F. Damjanić et al.), Pineridge Press, Swansea, 33-70.
Willam, K.J., Münz, T., Etse, G. and Menétrey, Ph. (1994) Failure conditions and localization in concrete, in **EURO-C 1994 Int. Conf. Computer Modelling of Concrete Structures** (eds H. Mang et al.), Pineridge Press, Swansea, 263-282.